Proceedings of the ASME 2020 Heat Transfer Summer Conference
SHTC2020

SHTC2020-8926 (11278)

VALIDATION OF AN ENHANCED DISPERSION ALGORITHM FOR USE WITH THE STATISTICAL PHONON TRANSPORT MODEL

Michael P. Medlar[1], Edward C. Hensel
Rochester Institute of Technology, Rochester, NY, USA

ABSTRACT

Computer simulations of quasi-particle based phonon transport in semiconductor materials rely upon numerical dispersion relations to identify and quantify the discrete energy and momentum states allowable subject to quantum constraints. The accuracy of such computer simulations is ultimately dependent upon the fidelity of the underlying dispersion relations. Dispersion relations have previously been computed using empirical fits of experimental data in high symmetry directions, lattice dynamics, and Density Function Theory (DFT) or Density Functional Perturbation Theory (DFPT) approaches. The current work presents high fidelity dispersion relations describing full anisotropy for all six phonon polarizations with an adjustable computational grid. The current approach builds upon the previously published Statistical Phonon Transport Model (SPTM), which employed a first nearest neighbor lattice dynamics approach for the dispersion calculation. This paper extends the lattice dynamics approach with the use of both first and second nearest neighbors interactions that are quantified using published interatomic force constants calculated from DFT. The First Brillouin Zone (FBZ) is segmented into eight octants of high symmetry, and discretized in wave vector space with a 14 by 14 by 14 grid. This results in 65,586 states of unique wave vector and frequency combinations. Dispersion calculations are performed at each of the six faces of the wave vector space volume elements in addition to the centroid, resulting in 460,992 solutions of the characteristic equations. For the given grid, on the order of 10^8 computations are required to compute the dispersion relations. The dispersion relations thus obtained are compared to experimental reports available for high symmetry axes. Full anisotropic results are presented for all six phonon polarizations across the range of allowable wave vector magnitude and frequency as a comprehensive model of allowable momentum and energy states. Results indicate excellent agreement to experiment in high symmetry directions for all six polarizations and illustrate an improvement as compared to the previous SPTM implementation. Dispersion relations based on the lattice dynamic model with first and second nearest neighbor atomic interactions relying upon DFT calculated inter-atomic force constants provides an accurate high fidelity energy and momentum model for use in phonon transport simulations.

Keywords: Phonon Transport, Lattice Dynamics, Dispersion Relations, SPTM

NOMENCLATURE

a	Acceleration or lattice constant
k	Wave vector
m	Mass
r	Position vector
u	Atomic displacement from equilibrium
x	Cartesian coordinate direction
y	Cartesian coordinate direction
z	Cartesian coordinate direction
A	Amplitude of atomic displacement
F	Force
M	Atomic mass
V	Interatomic potential
α	On site or first nearest neighbor force constant
β	First nearest neighbor force constant
δ	Second nearest neighbor force constant
λ	Second nearest neighbor force constant
μ	Second nearest neighbor force constant
ν	Second nearest neighbor force constant
ω	Angular frequency

1. INTRODUCTION

Dispersion curves show the available energy levels for phonons and the relationship between momentum and energy. Accurate determination of the dispersion relationships is vital as they affect the interaction among phonon modes that take place in three phonon scattering as well as the average speed that phonon wave packets travel through the physical domain.

[1] Contact author: mpmmet@rit.edu

Quasi-particle based phonon transport simulations, like those of the Monte-Carlo technique, have treated dispersion with varying levels of detail. Initial works gave all phonons the same group velocity and did not consider different polarizations [1]. Improvements were made to account for non-linear dispersion of acoustic phonons in an isotropic manner [2]. Curve fits to experimental dispersion data were implemented in an isotropic manner [3]. More recent work has used realistic dispersion relations calculated from the adiabatic bond charge model [4] or interatomic force constants from density functional theory [5]. This work builds upon the dispersion relations employed in the previously published Statistical Phonon Transport Model (SPTM) [6-8]. The lattice dynamics approach is extended to include both first and second nearest neighbor interactions. The interatomic interactions are quantified with published force constants calculated from Density Functional Theory [9, 10]. Full anisotropic results are computed for the all the acoustic and optical polarizations across the range of allowable wavevectors. The dispersion relations show excellent agreement to experimental results in high symmetry directions and provide for high fidelity phonon transport modeling with the SPTM.

2. METHODS

2.1 THEORY. This work makes use of the lattice dynamics technique with the harmonic assumption to calculate dispersion relations [11, 12]. This technique amounts to the application of Newton's second law to the atomic lattice where interatomic forces are expressed as a function of interatomic force constants and atomic displacements. Solutions to the system of equations that take the form of normal modes of vibration with a given frequency are found. The difficulty in the use of this method to obtain accurate results lies in the use of accurate interatomic force constants and the inclusion of enough neighboring interactions to reproduce the relevant physics. This model makes use of interatomic force constants calculated from Density Functional Theory (DFT) [9] and includes up to second nearest neighbor interactions.

Development of the model follows closely that of Herman [11]. For illustration, the relative arrangement of the first and second nearest neighbor atoms of silicon are shown below. The two atoms that make up the basis of silicon are illustrated with the box. If these atoms are applied to the Face-Centered-Cubic (FCC) lattice, then the diamond lattice is created.

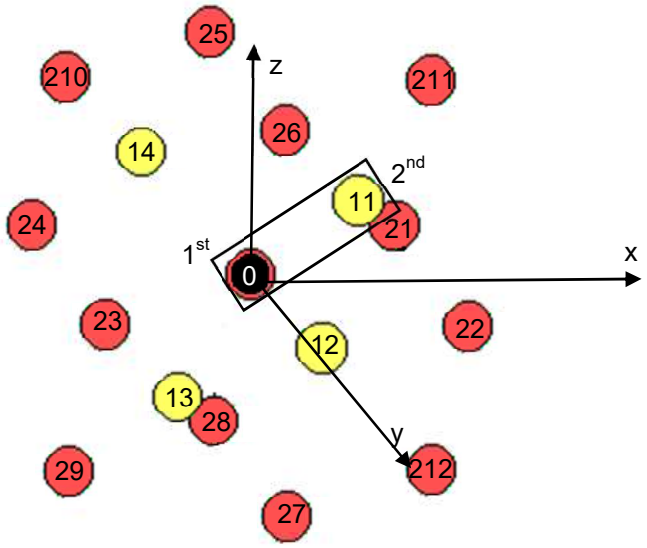

FIGURE 1: SILICON ATOMIC LATTICE. FIRST AND SECOND NEAREST NEIGHBORS. ADAPTED FROM [13].

The atoms in FIGURE 1 are labeled with the following scheme. The central atom is black and labeled as 0, the four nearest neighbor atoms are yellow and labeled 11-14, and the twelve second nearest neighbor atoms are red and labeled as 21 – 212. The derivation begins with application of Newton's second law to the central atom in each coordinate direction as follows:

$$\Sigma F_x = ma_x \tag{1}$$

$$\Sigma F_y = ma_y \tag{2}$$

$$\Sigma F_z = ma_z \tag{3}$$

An expanded version of the forces acting in the x-direction on atom 0 is shown in equation 4.

$$\begin{aligned}\sum F_x(0) = {} & F_x(00x) + F_x(00y) + F_x(00z) + \\ & F_x(011x) + F_x(012x) + F_x(013x) + \\ & F_x(014x) + F_x(011y) - F_x(012y) + \\ & F_x(013y) - F_x(014y) + F_x(011z) - \\ & F_x(012z) + F_x(013z) - F_x(014z) + \\ & F_x(021x) + F_x(022x) + F_x(023x) + \\ & F_x(024x) + F_x(025x) + F_x(026x) + \\ & F_x(027x) + F_x(028x) + F_x(029x) + \\ & F_x(0210x) + F_x(0211x) + F_x(0212x) + \\ & F_x(021y) + F_x(022y) + F_x(023y) + \\ & F_x(024y) + F_x(025y) + F_x(026y) + \\ & F_x(027y) + F_x(028y) + F_x(029y) + \\ & F_x(0210y) + F_x(0211y) + F_x(0212y) + \\ & F_x(021z) + F_x(022z) + F_x(023z) + \\ & F_x(024z) + F_x(025z) + F_x(026z) +\end{aligned}$$

$$F_x(027z) + F_x(028z) + F_x(029z) + F_x(0210z) + F_x(0211z) + F_x(0212z) \quad (4)$$

Each term represents the force resulting on atom 0 in the x direction when the given atom is displaced in a certain direction. For example, $F_x(011x)$ indicates the force in the x-direction on atom 0 when the atom labeled 11 is displaced in the x-direction. $F_x(027z)$ Indicates the force in the x-direction on atom 0 when atom 27 is displaced in the z-direction. Next, the forces acting on the atoms are expressed in terms of interatomic force constants multiplied by atomic displacements. This amounts to the harmonic assumption and will lead to reasonable results as deviation from equilibrium is relatively small for temperatures of interest to this work. This is expressed with equation 5,

$$F_x(011x) = \frac{\partial^2 V}{\partial x^2} u_{11x} \ , \quad (5)$$

where $\frac{\partial^2 V}{\partial x^2}$ is the second derivative of the interatomic potential between atom 0 and atom 11 and $u_{11x}$is the displacement of atom 11 in the x-direction. The second derivatives are the interatomic force constants and are traditionally expressed using the notion shown in TABLE 1.

TABLE 1: INTERATOMIC FORCE CONSTANTS [9]

α_0	On-site interaction
α_1	First nearest neighbors
β_1	
μ_2	Second nearest neighbors
ν_2	
δ_2	
λ_2	

Where a subscript of 0 indicates the original atom, a subscript of 1 indicates first nearest neighbors and 2 second nearest neighbors. The different force constants represent different interactions between the atoms involved. For example, α_1 represents the interaction between atom 0 in a given coordinate direction when the first nearest neighbors are displaced in the same directions. Thus, in equation 5, $\frac{\partial^2 V}{\partial x^2}$ is equal to α_1. Similarly, β_1 represents the interaction between atoms 0 in a given direction when the first nearest neighbors are displaced in orthogonal directions from atom 0. So, β_1 would appear in the equation for $F_x(011y)$ representing the second derivative term. Likewise, the second nearest neighbor force constants are used in a similar manner for the forces between atom 0 and the second nearest neighbor atoms labeled 21-212. However, the second nearest neighbor atoms form a different geometric configuration around atom 0 than compared to the first nearest neighbor atoms. Atoms 21 – 24 all lie in the x-y plane, atoms 25 – 28 lie in the y-z plane, and atoms 29 – 212 lie in the x-z plane. Because of this planar nature, four force constants are required to describe the interactions depending on whether the atoms are moved within the plane of the second nearest neighbors or out of the plane. μ_2 represents the force constant between atom 0 and atoms in the x-y and x-z planes when the atoms are displaced in the same in-plane coordinate direction. ν_2 represents the force constant between atom 0 and atoms in x-y and x-z planes when the atoms are moved in the orthogonal in-plane direction. δ_2 represents the force constant between atom 0 and the atoms in the x-y and y-z planes when they are moved in the orthogonal out-of-plane direction. λ_2 represents the force constant between atom 0 and the atoms in the y-z plane when they are moved in the same coordinate, out-of-plane, direction. The force constants above are obtained from the use of a first principles quantum electronic configuration calculation called DFT. For reference on DFT, please refer to Sholl [14].

After insertion of the force constant notation, the sum of the forces acting in the x-direction on atom 0 is shown with equation 6.

$$\begin{aligned} &-\alpha_0 u_x(0) - \alpha_1 u_x(11) - \alpha_1 u_x(12) - \\ &\alpha_1 u_x(13) - \alpha_1 u_x(14) - \beta_1 u_y(11) + \\ &\beta_1 u_y(12) + \beta_1 u_y(13) - \beta_1 u_y(14) - \\ &\beta_1 u_z(11) + \beta_1 u_z(12) - \beta_1 u_z(13) + \\ &\beta_1 u_z(14) - \mu_2 u_x(21) - \mu_2 u_x(22) - \\ &\mu_2 u_x(23) - \mu_2 u_x(24) - \lambda_2 u_x(25) - \\ &\lambda_2 u_x(26) - \lambda_2 u_x(27) - \lambda_2 u_x(28) - \\ &\mu_2 u_x(29) - \mu_2 u_x(210) - \mu_2 u_x(211) - \\ &\mu_2 u_x(212) + \nu_2 u_y(21) - \nu_2 u_y(22) + \\ &\nu_2 u_y(23) - \nu_2 u_y(24) + \nu_2 u_y(29) - \\ &\nu_2 u_y(210) + \nu_2 u_y(211) - \nu_2 u_y(212) - \\ &\delta_2 u_z(21) - \delta_2 u_z(22) + \delta_2 u_z(23) + \\ &\delta_2 u_z(24) - \delta_2 u_z(29) + \delta_2 u_z(210) - \\ &\delta_2 u_z(211) + \delta_2 u_z(212) = M_0 \ddot{u_x}(0) \end{aligned} \quad (6)$$

The atomic displacements are assumed to take the form of a wave solution. This can be thought of as a travelling wave moving through the lattice. An example of the displacement of atom 0 in the x-direction is shown with equation 7,

$$u_x(0) = A_x(0) e^{i\left(\omega t - \vec{k}\cdot\vec{r}(0)\right)} \ , \quad (7)$$

where $A_x(0)$ is the amplitude of the displacement of atom 0 in the x-direction, ω is the angular frequency of the wave, $\vec{k}$ is the wavevector and $\vec{r}(0)$ is the postion vector to atom 0. Upon insertion into the equations of motion, the following characteristic equation emerges.

$$\begin{aligned} &\alpha_0 A_x(0) + \alpha_1 A_x(1)\left[e^{-iK\cdot r(11)} + e^{-iK\cdot r(12)} + \right. \\ &\left. e^{-iK\cdot r(13)} + e^{-iK\cdot r(14)}\right] + \beta_1 A_y(1)\left[e^{-iK\cdot r(11)} - \right. \\ &\left. e^{-iK\cdot r(12)} - e^{-iK\cdot r(13)} + e^{-iK\cdot r(14)}\right] + \end{aligned}$$

$$\beta_1 A_z(1)\left[e^{-i\ \cdot r(11)} - e^{-iK\cdot r(12)} + e^{-i\ \cdot r(13)} - e^{-i\ \cdot r(14)}\right] + \mu_2 A_x(0)\left[e^{-iK\cdot r(21)} + e^{-iK\cdot r(22)} + e^{-iK\cdot r(23)} + e^{-iK\cdot r(24)} + e^{-iK\cdot r(29)} + e^{-iK\cdot r(210)} + e^{-iK\cdot r(211)} + e^{-iK\cdot r(212)}\right] + \lambda_2 A_x(0)\left[e^{-i(K\cdot r(25))} + e^{-i(K\cdot r(26))} + e^{-i(K\cdot r(27))} + e^{-i(K\cdot r(28))}\right] + \nu_2 A_y(0)\left[-e^{-i\ \cdot r(21)} + e^{-iK\cdot r(22)} - e^{-iK\cdot r(23)} + e^{-iK\cdot r(24)} - e^{-iK\cdot r(29)} - e^{-iK\cdot r(210)} + e^{-iK\cdot r(211)} + e^{-iK\cdot r(212)}\right] + \delta_2 A_z(0)\left[e^{-iK\cdot r(21)} + e^{-iK\cdot r(22)} - e^{-iK\cdot r(23)} - e^{-iK\cdot r(24)} + e^{-iK\cdot r(29)} - e^{-i\ \cdot r(210)} + e^{-iK\cdot r(211)} - e^{-iK\cdot r(212)}\right] = M_0\omega^2 A_x(0) \quad (8)$$

The terms have been grouped in terms of the amplitude of displacements of atom 0 and atom 1 in the x, y, and z directions. Atom 0 is the first basis atom in the silicon lattice and atom 1 is the second basis atom. Note that the second nearest neighbor atoms will share the same amplitude of displacements as the atom labeled 0 as they are identical by symmetry arguments. If the equations of motion are applied in this manner to the y and z directions to both the first and second basis atoms, six equations will result with six unknown displacement amplitudes. This sets up a system of equations that are shown in matrix form in equation 9,

$$\begin{bmatrix} A & B & C & D & E & F \\ G & H & I & E & D & L \\ M & N & O & F & L & D \\ D^* & E^* & F^* & A & B & C \\ E^* & D^* & L^* & G & H & I \\ F^* & L^* & D^* & M & N & O \end{bmatrix} \begin{bmatrix} A_x(0) \\ A_y(0) \\ A_z(0) \\ A_x(1) \\ A_y(1) \\ A_z(1) \end{bmatrix} = \begin{bmatrix} A_x(0)M\omega^2 \\ A_y(0)M\omega^2 \\ A_z(0)M\omega^2 \\ A_x(1)M\omega^2 \\ A_y(1)M\omega^2 \\ A_z(1)M\omega^2 \end{bmatrix}, \quad (9)$$

where the left hand six by six matrix is known as the dynamical matrix. Its coefficients contain all of the interatomic force constants above and are also a function of a given wavevector. A star (*) indicates the complex conjugate. The elements of the dynamical matrix are shown below.

$$A = \alpha_0 + \mu_2\left[4cos\left(\frac{a}{2}k_x\right)cos\left(\frac{a}{2}k_y\right) + 4cos\left(\frac{a}{2}k_x\right)cos\left(\frac{a}{2}k_z\right)\right] + \lambda_2\left[4cos\left(\frac{a}{2}k_y\right)cos\left(\frac{a}{2}k_z\right)\right] \quad (10)$$

$$B = \nu_2\left[-e^{-i\left(\frac{a}{2}(k_x-k_y)\right)} + e^{-i\left(\frac{a}{2}(k_x+k_y)\right)} - e^{-i\left(\frac{a}{2}(-k_x+k_y)\right)} + e^{-i\left(\frac{a}{2}(-k_x-k_y)\right)}\right] + \delta_2\left[-e^{-i\left(\frac{a}{2}(-k_y+k_z)\right)} - e^{-i\left(\frac{a}{2}(k_y+k_z)\right)} + e^{-i\left(\frac{a}{2}(k_y-k_z)\right)} + e^{-i\left(\frac{a}{2}(-k_y-k_z)\right)} - e^{-i\left(\frac{a}{2}(-k_x-k_z)\right)} + e^{-i\left(\frac{a}{2}(-k_x+k_z)\right)} + e^{-i\left(\frac{a}{2}(k_x+k_z)\right)} - e^{-i\left(\frac{a}{2}(k_x-k_z)\right)}\right] \quad (11)$$

$$C = \nu_2\left[e^{-i\left(\frac{a}{2}(-k_x-k_z)\right)} - e^{-i\left(\frac{a}{2}(-k_x+k_z)\right)} + e^{-i\left(\frac{a}{2}(k_x+k_z)\right)} - e^{-i\left(\frac{a}{2}(k_x-k_z)\right)}\right] + \delta_2\left[e^{-i\left(\frac{a}{2}(k_x-k_y)\right)} + e^{-i\left(\frac{a}{2}(k_x+k_y)\right)} + e^{-i\left(\frac{a}{2}(-k_x+k_y)\right)} + e^{-i\left(\frac{a}{2}(-k_x-k_y)\right)} + e^{-i\left(\frac{a}{2}(-k_y+k_z)\right)} - e^{-i\left(\frac{a}{2}(k_y+k_z)\right)} + e^{-i\left(\frac{a}{2}(k_y-k_z)\right)} - e^{-i\left(\frac{a}{2}(-k_y-k_z)\right)}\right] \quad (12)$$

$$D = 4\alpha_1 cos\left(\frac{a}{4}k_x\right)cos\left(\frac{a}{4}k_y\right)cos\left(\frac{a}{4}k_z\right) + i\left[4\alpha_1 sin\left(\frac{a}{4}k_x\right)sin\left(\frac{a}{4}k_y\right)sin\left(\frac{a}{4}k_z\right)\right] \quad (13)$$

$$E = \beta_1\left[e^{-i\left(\frac{a}{4}(k_x+k_y+k_z)\right)} - e^{-i\left(\frac{a}{4}(k_x-k_y-k_z)\right)} - e^{-i\left(\frac{a}{4}(-k_x+k_y-k_z)\right)} + e^{-i\left(\frac{a}{4}(-k_x-k_y+k_z)\right)}\right] \quad (14)$$

$$F = \beta_1\left[e^{-i\left(\frac{a}{4}(k_x+k_y+k_z)\right)} - e^{-i\left(\frac{a}{4}(k_x-k_y-k_z)\right)} + e^{-i\left(\frac{a}{4}(-k_x+k_y-k_z)\right)} - e^{-i\left(\frac{a}{4}(-k_x-k_y+k_z)\right)}\right] \quad (15)$$

$$G = \nu_2\left[-e^{-i\left(\frac{a}{2}(k_x-k_y)\right)} + e^{-i\left(\frac{a}{2}(k_x+k_y)\right)} - e^{-i\left(\frac{a}{2}(-k_x+k_y)\right)} + e^{-i\left(\frac{a}{2}(-k_x-k_y)\right)}\right] + \delta_2\left[e^{-i\left(\frac{a}{2}(-k_y+k_z)\right)} + e^{-i\left(\frac{a}{2}(k_y+k_z)\right)} - e^{-i\left(\frac{a}{2}(k_y-k_z)\right)} - e^{-i\left(\frac{a}{2}(-k_y-k_z)\right)} + e^{-i\left(\frac{a}{2}(-k_x-k_z)\right)} - e^{-i\left(\frac{a}{2}(-k_x+k_z)\right)} - e^{-i\left(\frac{a}{2}(k_x+k_z)\right)} + e^{-i\left(\frac{a}{2}(k_x-k_z)\right)}\right] \quad (16)$$

$$H = \alpha_0 + \mu_2\left[4cos\left(\frac{a}{2}k_x\right)cos\left(\frac{a}{2}k_y\right) + 4cos\left(\frac{a}{2}k_y\right)cos\left(\frac{a}{2}k_z\right)\right] + \lambda_2\left[4cos\left(\frac{a}{2}k_x\right)cos\left(\frac{a}{2}k_z\right)\right] \quad (17)$$

$$I = \nu_2\left[-e^{-i\left(\frac{a}{2}(-k_y+k_z)\right)} + e^{-i\left(\frac{a}{2}(k_y+k_z)\right)} - e^{-i\left(\frac{a}{2}(k_y-k_z)\right)} + e^{-i\left(\frac{a}{2}(-k_y-k_z)\right)}\right] + \delta_2\left[e^{-i\left(\frac{a}{2}(k_x-k_y)\right)} + e^{-i\left(\frac{a}{2}(k_x+k_y)\right)} -\right.$$

$$e^{-i\left(\frac{a}{2}(-k_x+k_y)\right)} - e^{-i\left(\frac{a}{2}(-k_x-k_y)\right)} + e^{-i\left(\frac{a}{2}(-k_x-k_z)\right)} + e^{-i\left(\frac{a}{2}(-k_x+k_z)\right)} - e^{-i\left(\frac{a}{2}(k_x+k_z)\right)} - e^{-i\left(\frac{a}{2}(k_x-k_z)\right)}\Big] \quad (18)$$

$$L = \beta_1\left[e^{-i\left(\frac{a}{4}(k_x+k_y+k_z)\right)} + e^{-i\left(\frac{a}{4}(k_x-k_y-k_z)\right)} - e^{-i\left(\frac{a}{4}(-k_x+k_y-k_z)\right)} - e^{-i\left(\frac{a}{4}(-k_x-k_y+k_z)\right)}\right] \quad (19)$$

$$M = \nu_2\left[e^{-i\left(\frac{a}{2}(-k_x-k_z)\right)} - e^{-i\left(\frac{a}{2}(-k_x+k_z)\right)} + e^{-i\left(\frac{a}{2}(k_x+k_z)\right)} - e^{-i\left(\frac{a}{2}(k_x-k_z)\right)}\right] + \delta_2\left[e^{-i\left(\frac{a}{2}(k_x-k_y)\right)} - e^{-i\left(\frac{a}{2}(k_x+k_y)\right)} - e^{-i\left(\frac{a}{2}(-k_x+k_y)\right)} + e^{-i\left(\frac{a}{2}(-k_x-k_y)\right)} - e^{-i\left(\frac{a}{2}(-k_y+k_z)\right)} + e^{-i\left(\frac{a}{2}(k_y+k_z)\right)} + e^{-i\left(\frac{a}{2}(k_y-k_z)\right)} - e^{-i\left(\frac{a}{2}(-k_y-k_z)\right)}\right] \quad (20)$$

$$N = \nu_2\left[-e^{-i\left(\frac{a}{2}(-k_y+k_z)\right)} + e^{-i\left(\frac{a}{2}(k_y+k_z)\right)} - e^{-i\left(\frac{a}{2}(k_y-k_z)\right)} + e^{-i\left(\frac{a}{2}(-k_y-k_z)\right)}\right] + \delta_2\left[-e^{-i\left(\frac{a}{2}(k_x-k_y)\right)} - e^{-i\left(\frac{a}{2}(k_x+k_y)\right)} + e^{-i\left(\frac{a}{2}(-k_x+k_y)\right)} + e^{-i\left(\frac{a}{2}(-k_x-k_y)\right)} - e^{-i\left(\frac{a}{2}(-k_x-k_z)\right)} - e^{-i\left(\frac{a}{2}(-k_x+k_z)\right)} + e^{-i\left(\frac{a}{2}(k_x+k_z)\right)} + e^{-i\left(\frac{a}{2}(k_x-k_z)\right)}\right] \quad (21)$$

$$O = \alpha_0 + \mu_2\left[4cos\left(\frac{a}{2}k_y\right)cos\left(\frac{a}{2}k_z\right) + 4cos\left(\frac{a}{2}k_x\right)cos\left(\frac{a}{2}k_z\right)\right] + \lambda_2\left[4cos\left(\frac{a}{2}k_x\right)cos\left(\frac{a}{2}k_y\right)\right] \quad (22)$$

For a given wavevector, there exist six solutions for the frequency that satisfy the equations of motion. These are the eigenvalues of the dynamical matrix and represent the six phonon modes (or polarizations). They consist of the two transverse acoustic (TA1, TA2), the longitudinal acoustic (LA), the two transverse optical (TO1, TO2), and the longitudinal optical (LO) mode (or polarization).

2.2 IMPLEMENTATION. The lattice dynamics model described in the preceding section can be used to calculate the frequencies of the six modes corresponding to any given wavevector. Within the SPTM, it is implemented on a uniform discretization of wavevector (k) space. This paper uses a mesh size of 14 but it is recognized that results can be sensitive to the chosen mesh size. For the proposal, a mesh size of 14 implies that the principle directions within the wavevector space are divided into 14 equal sized elements. This is shown in three dimensions for one eighth (one octant) of the FBZ with the FIGURE 2.

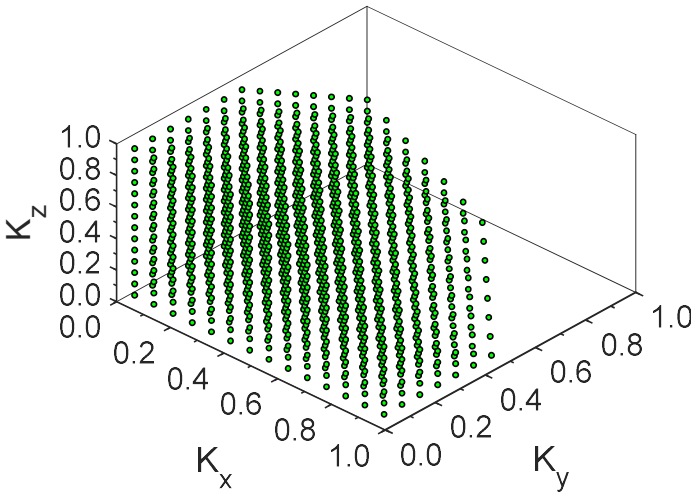

FIGURE 2: DISCRETIZATION OF ONE OCTANT OF WAVEVECTOR SPACE FOR A MESH SIZE OF 14.

The k-space elements are labeled by the location of their centroids. With the mesh size chosen, there are 10,976 elements in the FBZ. The lattice dynamics model is applied to calculate the six representative frequencies at the centroids of the elements. The wavevector and frequency values associated with the centroid points are used as labels and unique combinations of wavevector centroid and calculated frequency are referred to as pseudo-states. There are 65,856 pseudo-states in the FBZ for the chosen mesh size. For a mesh size of 12 there are 41,472 pseudo-states and for a mesh size of 16 there are 98,304 pseudo-states. Dispersion calculations are performed at each of the six faces of the wavevector space volume elements in addition to the centroid. Thus, for an implementation of the dispersion calculation on a mesh size of 14, there are seven solutions of equation 19 generated in complex double precision for each of the 65,856 pseudo-states. This results in 460,992 instances of Equation 19 that are solved through the use of the GNU Scientific Library (GSL) open source software package [15]. This package contains a complex eigenvalue solver. The GSL complex eigenvalue solver uses the complex form of the symmetric bi-diagonalization and QR reduction method. This method is assumed to take on the order of N^3 calculations [16]. Thus for the mesh size of 14, on the order of 10^8 computations would be involved for the dispersion calculations.

Values of the interatomic force constants that were implemented in the solution of the dynamical matrix for the calculation of dispersion relationships in pure silicon are shown with TABLE 2. The values for germanium are shown as well and could be implemented to compute dispersion relations for pure germanium.

TABLE 2: INTERATOMIC FORCE CONSTANTS IN UNITS OF N/M [10]

	Silicon	Germanium
α_0	215.41173	185.33255
α_1	-52.54514	-45.88164
β_1	-36.64926	-32.63248
μ_2	-2.92696	-2.31977
ν_2	-2.83355	-2.10181
δ_2	1.72815	1.38563
λ_2	6.69464	6.00961

The value of μ_2 for silicon is adjusted to -4.001216 N/m to ensure enforcement of the acoustic sum rule. This rule implies the following when using interatomic force constants up to second nearest neighbors [17].

$$\alpha_0 = -4\alpha_1 - 8\mu_2 - 4\lambda_2 \quad (23)$$

The solutions from the dispersion calculations are stored for future use in both scattering and drift algorithms. The group velocities are calculated in each of the coordinate directions with knowledge of the frequencies and wavevectors. Group velocities are used when considering the drift (unimpeded movement) of phonons between different geometric cells. The wavevector and frequency will be used in both the selection of three phonon scattering partners and the calculation of the three phonon scattering rates.

3. RESULTS AND DISCUSSION

The lattice dynamics formulation previously implemented in the SPTM utilized only first nearest neighbor interactions and force constants reported by Ghatak and Kothari [18]. The results of this calculation, which were previously reported by Wang and Murthy [19] (and reproduced by Brown III [8]), show that at the worst case location (close to the X point) the prediction is off by about 75%. The results for the enhanced dispersion model implemented in this work compared to similar experimental data are shown in FIGURE 3.

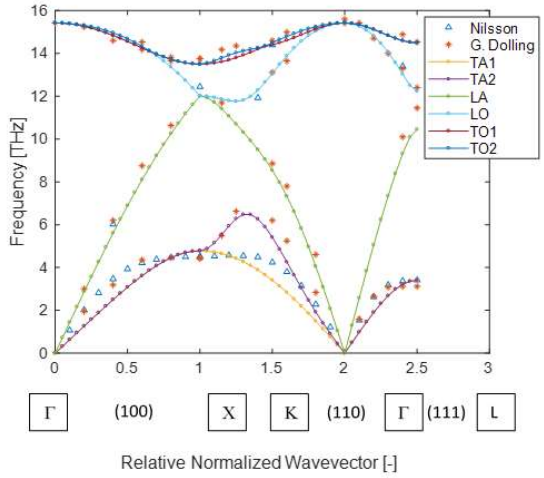

FIGURE 3: PREDICTED DISPERSION RESULTS FOR LATTICE DYNAMICS MODEL (WITH UP TO SECOND NEAREST NEIGHBOR INTERACTIONS AND FORCE CONSTANTS CALCULATED FROM FIRST PRINCIPLES DFT) COMPARED TO EXPERIMENTAL. THE PREDICTIONS ARE FOR 500 K AND THE DATA WAS TAKEN AT 300 K. THE TRIANGLES ARE FROM NILSSON AND NELIN [20] AND THE STARS ARE FROM G. DOLLING [21].

There is much better agreement in the high symmetry directions with the enhanced dispersion calculation of the SPTM. At the worst case location, the model predictions are only off by 19%. In addition to results in high symmetry directions, the SPTM calculations produce dispersion relations in all directions within the FBZ. This is in contrast to many MC simulations such as those of Pop et al. [22], Mittal et al. [23], and Hao et al. [24], where dispersion relations are assumed to be isotropic and are developed from either fits of experimental data in high symmetry directions or from simple sin-shaped functions. The results of the complete anisotropic dispersion calculation of the SPTM are shown in FIGURE 4.

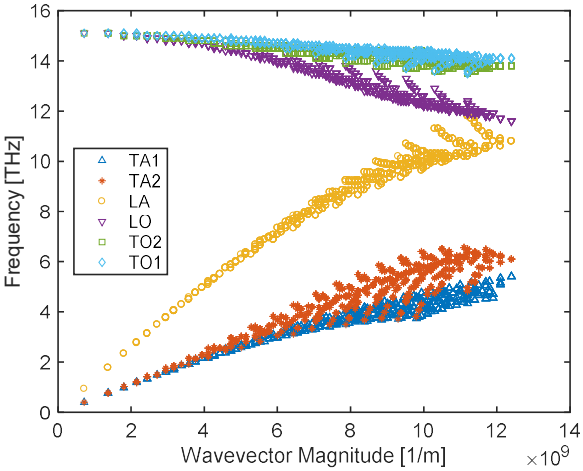

FIGURE 4: PREDICTED DISPERSION RESULTS FROM LATTICE DYNAMICS WITH SECOND NEAREST NEIGHBOR INTERACTIONS IN ALL MODELED DIRECTIONS IN THE FBZ. MESH SIZE OF 14. TEMPERATURE OF 500 K.

4. CONCLUSION

The lattice dynamics approach has been implemented to improve the computed dispersion relations utilized in the SPTM. The interactions are extended to include both first and second nearest neighbor interatomic influences. The force constants have been quantified with the use of the first principles electronic configuration calculations of DFT. The improved model shows excellent agreement to experiment in high symmetry directions and provides the foundation to a high fidelity phonon transport method.

ACKNOWLEDGEMENTS

The author would like to acknowledge useful e-mail communications from Dr. Kevian Esfarjani.

REFERENCES

[1] Peterson, R. B., 1994, "Direct Simulation of Phonon-Mediated Heat Transfer in a Debye Crystal," Journal of Heat Transfer, 116(4), pp. 815.
[2] Mazumder, S., and Majumdar, A., 2001, "Monte Carlo Study of Phonon Transport in Solid Thin Films Including Dispersion and Polarization," JOURNAL OF HEAT TRANSFER-TRANSACTIONS OF THE ASME, 123(4), pp. 749-759.
[3] Mittal, A., and Mazumder, S., 2010, "Monte Carlo Study of Phonon Heat Conduction in Silicon Thin Films Including Contributions of Optical Phonons," JOURNAL OF HEAT TRANSFER-TRANSACTIONS OF THE ASME, 132(5), pp. 52402.
[4] Kukita, K., and Kamakura, Y., 2013, "Monte Carlo Simulation of Phonon Transport in Silicon Including a Realistic Dispersion Relation," JOURNAL OF APPLIED PHYSICS, 114(15), pp. 154312.
[5] Wu, R., Hu, R., and Luo, X., 2016, "First-Principle-Based Full-Dispersion Monte Carlo Simulation of the Anisotropic Phonon Transport in the Wurtzite Gan Thin Film," Journal of Applied Physics, 119(14), pp. 145706.
[6] Brown, T. W., and Hensel, E., 2012, "Statistical Phonon Transport Model for Multiscale Simulation of Thermal Transport in Silicon: Part I – Presentation of the Model," International Journal of Heat and Mass Transfer, 55(25-26), pp. 7444-7452.
[7] Brown, T. W., and Hensel, E., 2012, "Statistical Phonon Transport Model for Multiscale Simulation of Thermal Transport in Silicon: Part Ii – Model Verification and Validation," International Journal of Heat and Mass Transfer, 55(25-26), pp. 7453-7459.
[8] Brown III, T. W., 2012, "A Statistical Phonon Transport Model for Thermal Transport in Crystalline Materials from the Diffuse to Ballistic Regime," Doctor of Philosophy Rochester Institute of Technology, Rochester, NY.
[9] Esfarjani, K., and Stokes, H. T., 2008, "Method to Extract Anharmonic Force Constants from First Principles Calculations," Physical Review B, 77(14).
[10] Aouissi, M., Hamdi, I., Meskini, N., and Qteish, A., 2006, "Phonon Spectra of Diamond, Si, Ge, and Alpha-Sn: Calculations with Real-Space Interatomic Force Constants," PHYSICAL REVIEW B, 74(5).
[11] Herman, F., 1959, "Lattice Vibrational Spectrum of Germanium," Journal of Physics and Chemistry of Solids, 8(pp. 405-418.
[12] Reissland, J. A., 1973, The Physics of Phonons, Wiley, London;New York;.
[13] Van Zeghbroeck, B. J., 1996, https://ecee.colorado.edu/~bart/book/eband3.htm
[14] Sholl, D., and Steckel, J. A., 2009, Density Functional Theory: A Practical Introduction, Wiley-Interscience, Hoboken.
[15] Galassi, M., and Gough, B., 2001, Gnu Scientific Library: Reference Manual, Network Theory, Bristol, UK.
[16] Vandebril, R., Barel, M. V., Mastronardi, N., and Proquest, 2008, Matrix Computations and Semiseparable Matrices, Johns Hopkins University Press, Baltimore.
[17] Aouissi, M., Hamdi, I., Meskini, N., and Qteish, A., 2006, "Phonon Spectra of Diamond, Si, Ge, Andα−Sn: Calculations with Real-Space Interatomic Force Constants," Physical Review B, 74(5).
[18] Ghatak, A. K., and Kothari, L. S., 1972, An Introduction to Lattice Dynamics, Addison-Wesley, London, Reading, Mass.,.
[19] Wang, T., and Murthy, J. Y., 2006, "Solution of the Phonon Boltzmann Transport Equation Employing Rigorous Implementation of Phonon Conservation Rules," Proc. ASME International Mechanical Engineering Congress and Exposition, Chicago, Illinois, USA.
[20] Nelin, G., and Nilsson, G., 1972, "Phonon Density of States in Germanium at 80 K Measured by Neutron Spectrometry," Physical Review B, 5(8), pp. 3151-3160.
[21] Dolling, G., and Cowley, A., 1966, Proc. Proc. Phys. Soc. London.
[22] Pop, E., Dutton, R. W., and Goodson, K. E., 2004, "Analytic Band Monte Carlo Model for Electron Transport in Si Including Acoustic and Optical Phonon Dispersion," Journal of Applied Physics, 96(9), pp. 4998-5005.
[23] Mittal, A., and Mazumder, S., 2010, "Monte Carlo Study of Phonon Heat Conduction in Silicon Thin Films Including Contributions of Optical Phonons," Journal of Heat Transfer, 132(5), pp. 52402.
[24] Hao, Q., Zhao, H., and Xiao, Y., 2017, "A Hybrid Simulation Technique for Electrothermal Studies of Two-Dimensional Gan-on-Sic High Electron Mobility Transistors," Journal of Applied Physics, 121(20), pp. 204501.